VŠB – Technická univerzita Ostrava

Univerzitní studijní programy

Barevné efekty v optické spektroskopii

Color Effects in Optical Spectroscopy

Author: Šárka Kunčická

Supervisor: doc. Dr. Mgr. Kamil Postava

Ostrava 2014

VŠB - Technical University of Ostrava
University Study Programmes
Institute of Physics

Bachelor Thesis Assignment

Student:	**Šárka Kunčická**
Study Programme:	B3942 Nanotechnology
Study Branch:	3942R001 Nanotechnology
Title:	Barevné efekty v optické spektroskopii Color effects in optical spectroscopy

Zásady pro vypracování:

Cílem práce je vypočítat z měřených a modelovaných optických spekter barvu popsanou barevnými souřadnicemi např. CIE xyz, RGB, CMYK, zvládnout přepočet barevných souřadnic a vykreslení barev. Modelování spekter vychází z elektromagnetické optiky se započtením odpovídajících hraničních podmínek, měřená spektra budou získávána na elipsometru Woollam RC2. Bakalářská práce bude obsahovat tyto části:

1. Výpočet barevných souřadnic z optických spekter (rešerše literatury, teorie)
2. Popis barevných jevů v přírodě, atmosferická optika (návaznost na stáž Umea University, Švédsko)
3. Barevné efekty při odrazu od tenkých vrstev, barvy a spektroskopická polarimetrie Muellerovy matice, vliv difrakce.

Description:

The main target of the bachelor thesis is to calculate colors from measured and modeled optical spectra. The color is described by trichromatic coordinates, i.e., CIE xyz, RGB, CMYK. Spectra modeling is based on electromagnetic optics with including appropriate boundary conditions. Measured spectra are obtained from the ellipsometer Woollam RC2. Thesis will consist of three parts:

1. Calculation of trichromatic coordinates from optical spectra (theory, literature recherche).
2. Color effects in nature, atmospheric optics (related to stay in Umea University, Sweden).
3. Color effects by reflection from thin films, color and spectroscopic Mueller matrix polarimetry, diffraction.

References:

[1] D. Malacara, Color Vision and Colorimetry, Theory and Applications, SPIE Press, 2002.
[2] H. Fujiwara, Spectroscopic Ellipsometry: Principles and Applications, Willey, 2007.
[3] G. P. Konnen, Polarized light in nature, Cambridge University Press 1985.
[4] B. A. Saleh, M. C. Teich, Fundamentals of Photonics, Wiley, 2007.
[5] P. Yeh, Optical Waves in Layered Media, Willey, 1988.

Extent and terms of a thesis are specified in directions for its elaboration that are opened to the public on the web sites of the faculty.

Supervisor: **doc. Dr.Mgr. Kamil Postava**

Date of issue:

Date of submission:

Prof. Dr.RNDr. Jiří Luňáček
Head of Department

prof. Ing. Petr Noskievič, CSc.
Vice-rector for Study Affairs

Declaration

I declare I have elaborated this thesis by myself. All literary references and publications I have used had been cited.

Ostrava, May 15, 2014 .....

Šárka Kunčická

Prohlášení

- Byla jsem seznámena s tím, že na moji bakalářskou práci se plně vztahuje zákon č.121/2000 Sb. – autorský zákon, zejména § 35 – využití díla v rámci občanských a náboženských obřadů, v rámci školních představení a využití díla školního a § 60 – školní dílo.
- Beru na vědomí, že Vysoká škola báňská – Technická univerzita Ostrava (dále jen VŠB-TUO) má právo nevýdělečně, ke své vnitřní potřebě, bakalářskou práci užít (§ 35 odst. 3).
- Souhlasím s tím, že jeden výtisk bakalářské práce bude uložen v Ústřední knihovně VŠB-TUO k prezenčnímu nahlédnutí a jeden výtisk bude uložen u vedoucího bakalářské práce. Souhlasím s tím, že údaje o bakalářské práci, obsažené v Záznamu o zveřejněné práci, umístěném v příloze mé bakalářské práce, budou zveřejněny v informačním systému VŠB-TUO.
- Bylo sjednáno, že s VŠB-TUO, v případě zájmu z její strany, uzavřu licenční smlouvu s oprávněním užít dílo v rozsahu § 12 odst. 4 autorského zákona.
- Bylo sjednáno, že užít své dílo – bakalářskou práci nebo poskytnout licenci k jejímu využití mohu jen se souhlasem VŠB-TUO, která je oprávněna v takovém případě ode mne požadovat přiměřený příspěvek na úhradu nákladů, které byly VŠB-TUO na vytvoření díla vynaloženy (až do jejich skutečné výše).
- Beru na vědomí, že odevzdáním své práce souhlasím se zveřejněním své práce podle zákona č. 111/1998 Sb., o vysokých školách a o změně a doplnění dalších zákonů (zákon o vysokých školách), ve znění pozdějších předpisů, bez ohledu na výsledek její obhajoby.

V Ostravě 15. 5. 2014

Šárka Kunčická

Šárka Kunčická

Adresa trvalého pobytu: Hlavní třída 564, Ostrava – Poruba, 708 00

Acknowledgement

I would like to express my deep gratitude to my supervisor doc. Dr. Mgr. Kamil Postava for his guidance, motivation, inspirational ideas, will and finally his admirable patience during a troubleshooting with the organization of the thesis, calculations and programming.

Furthermore, I would like to thank Ing. Lukáš Halagačka for his advice, insights and helping with coding in MATLAB.

ABSTRAKT

Hlavním cílem této bakalářské práce je výpočet barev z měřených a modelovaných optických spekter. Pro detailní popis barvy jsou vybrány barevné prostory CIE XYZ, RGB. V práci jsou uvedeny hlavní optické principy atmosférické optiky a některé optické jevy včetně polární záře, ze které jsou vypočteny barevné souřadnice, což je původním výsledkem této práce. Barevné efekty při odrazu světla od tenkých vrstev jsou také znázorněny. Modelování spekter tenkých vrstev vychází z elektromagnetické optiky, maticového popisu tenkých vrstev a optických konstant daného materiálu. Naměřená spektra jsou získána pomocí elipsometru Woollam RC2. Vypočtené spektrální křivky popisující barvu objektu jsou získány z experimentálně naměřených a modelovaných spekter na tepelně vypěstovaných SiO_2 vrstvách na křemíkovém podkladu.

Klíčová slova: barva, spektra, tenké vrstvy, CIE XYZ, RGB, atmosferické jevy, aurora, chromatické souřadnice, chromatický diagram, elipsometrie

Bibliografická citace:

Kunčická, Š. Barevné efekty v optické spektroskopii. Bakalářská práce, Vysoká škola báňská – Technická univerzita Ostrava, Univerzitní studijní programy, Institut fyziky, Ostrava. 2014.

ABSTRACT

The main aim of this bachelor thesis is to calculate colors from measured and modeled optical spectra. For describing a color in details, the color spaces CIE XYZ, RGB are selected. The main optical principles of the atmospheric optics and some optical phenomena are described, including the Aurora Borealis (Northern lights) chromaticity coordinates of which are calculated. The color effects by reflection of thin films are shown as well. A thin film spectra modeling is based on the electromagnetic optics, matrix description of thin films and optical constants of a given material. Measured spectra are obtained from the Woollam RC2 ellipsometer. The calculated trichromatic coordinates are obtained from experimentally measured and modeled spectra on thermally grown SiO_2 films on silicon wafers.

Key words: color, spectra, thin film, CIE XYZ, RGB, atmospheric phenomena, aurora, chromaticity coordinates, chromaticity diagram, ellipsometry

Reference format:

Kunčická, Š. Color Effects in Optical Spectroscopy. Bachelor thesis, VŠB – Technical University of Ostrava, University Study Programmes, Institute of Physics, Ostrava. 2014.

CONTENTS

1. INTRODUCTION

A motivation to write this thesis comes from my interest in atmospheric optics related with color effects and description of color effects for applications of thin films and periodic systems. The atmospheric optics brings an explanation of color effects occurring in nature and the optical spectroscopy enables to examine thin films in terms of color effects caused by reflection of light from them and interference phenomena. Looking on a surface of a thin film by a human eye, colors similar to those in the atmospheric phenomena can be seen. The main goal is to find a relation between those two fields.

Nowadays, it is possible to measure or model optical spectra of thin films and also to measure those of the atmospheric phenomena. The colorimetry, a science of color measurement, determines the color spaces, enables to calculate and display the chromaticity coordinates of thin films of other phenomena. The trichromatic coordinates are calculated from the tristimulus values and the color-matching functions given by specific color spaces (CIE XYZ, RGB etc.). Proper understanding of the color description is essential for proper color display, printing and design of advanced color surfaces.

Therefore, this thesis brings a connection of the color optics with the atmospheric optics and the color optical spectroscopy by the trichromatic coordinates resulting from the colorimetry.

The thesis is organized as follows: In the second chapter, the fundamentals of colorimetry are shown together with calculations important for modeling of colors and calculating the color effects of thin films or an aurora. A possibility of a transformation of one color space into another is shown here. The third chapter outlines a variety of optical phenomena in nature, from those caused by the main optical principles to the aurora caused by principles of particle physics but with a great optical spectral range during its displaying. From the values of auroral optical spectrum the calculation were performed. The same calculating procedure is used for calculating the trichromatic coordinates from thin film optical spectra. The fourth chapter outlines the main usage of thin films, their definition and characterization, describes a thin film spectrum and its measurement and calculation. The measuring method – ellipsometry is described as well. There is also an experimental part where the modeled reflection spectra of thin films are compared to those obtained by the measurement, as well as the graphically processed results.

2. COLORS IN OPTICAL SPECTROSCOPY – CALCULATION OF TRICHROMATIC COORDINATES FROM OPTICAL SPECTRA

2.1. Electromagnetic Spectrum – Visible Part

Each human being is exposed every day to different types of electromagnetic radiation, from the low - frequency radio waves to highest photon energy radiation of gamma rays. The types of those radiations are gathered to the electromagnetic spectrum which reflects the wide range of frequencies. The electromagnetic spectra include seven typical spectral ranges. They are sorted from the lowest frequency radiation mentioned above, across the microwaves, infrared, visible and ultraviolet spectrum to X-ray and gamma radiation. All of those electromagnetic waves travel with the same speed in vacuum – the speed of light *c*. Each of them may be characterized by its wavelength, in air or in vacuum, the frequency *ν,* and the photon energy *E*. The equations which relate these quantities are $\lambda_{vac} = \frac{c}{\nu}$ and $E = h \cdot \nu = \frac{h \cdot c}{\lambda}$. The various spectral regions differ in wavelength and frequency, thus affects substantially their detection and interaction with matter. The visible part of the electromagnetic spectrum is fundamental for this bachelor thesis [1, 2].

The visible spectrum (color spectrum) is a visible part of the electromagnetic spectrum which spreads through the wavelengths from approximately 380 nm to 780 nm. The light of different wavelengths produces different sense of color. Longer wavelengths produce the perception of red color while shorter wavelengths are blue to violet. Single wavelength produces pure color. This spectrum can be detected by the human eye. The eye is the most sensitive to photons with wavelengths around 580 nm because the wavelength corresponds to the color of the Sun. The orange color has then the wavelength of 600 nm. The wavelengths of other individual spectral colors are about 450 nm for blue color, 520 nm for green and 650 nm for red color [3]. The pure color spectrum does not contain all the colors that we are able to distinguish by eye and brain. All unsaturated colors like pink or magenta are absent because they are a mixture of multiple wavelengths. The saturation is given by mixture of red and white color since red is 100% saturated and white is 0% saturated. So colors obtained by mixing the saturated color with white are said to have the same hue but dispose of different saturation. The degree of saturation is called chroma and tells us how much the color is saturated. Hence, the relative amount of mixture of colors (saturated one with white) is determined by the color saturation, or chroma [4].

The wavelength of light from any part of the spectrum that passes through a medium decreases by dividing by refractive index of that medium. The values of wavelength are usually measured in vacuum or in air [5].

There could be exactly three various types of visible spectra with noticeably difference between them which is shown in Figure 1.

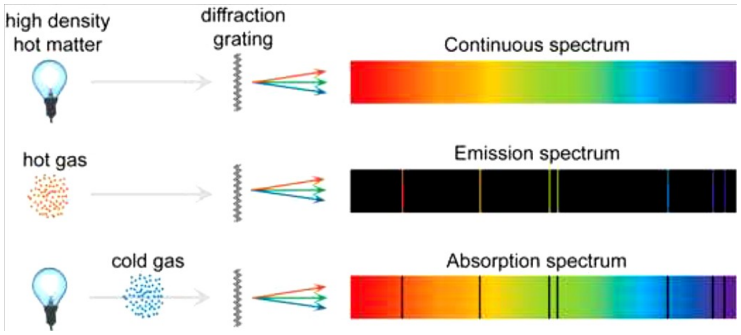

Fig. 1: Types of the visible spectra [6].

There is continuous spectrum, emission spectrum and absorption spectrum. In optical spectroscopy, more precisely in measuring color and its coordinates, all color effects take place in the continuous spectrum. This spectrum is connected also to atmospheric optics. However, the visible spectrum of an aurora phenomenon has the character of emission spectrum because the spectrum is formed from colors emitted by various atoms of gases in an outer atmosphere of the Earth and the spectral lines are characteristic for each element, found in the atmosphere. The absorption spectra occur when the atoms of cold gas absorb the characteristic frequencies and cause the absence of light in visible spectrum (absorption lines).

2.2. Color Vision

Color vision can be basically considered as the function of three sensors. There are three different types of cones in the human eye so it is expected that the evaluation of a color from spectral power data will result in three diverse reactions. The basis chosen is three-color matching or trichromatic matching, as it is usually called. For trichromatic matching functions to form a proper basis for a system of color measurement, various parts of the experimental system must be precisely specified, as well as the colors of the red, green and blue matching stimuli [5].

2.2.1. Standard Colorimetric Observer

The retina differs extensively in its characteristics from one part to another and it is necessary to specify the angle of the matching field. There are two field sizes exsisting, 2° and 10°, but the original CIE system was based on the 2° field of view [5]. These conceptions can be found under the terms „CIE 1931 Standard Colorimetric Observer" and „CIE 1964 Standard Colorimetric Observer" [5, 7]. The first one is proposed for an interface with visual color matching of fields of angular subtense between 1°and approximately 4°at the eye of the observer. A 2° field of view has a diameter of 17 mm at a viewing distance of 0.5 m. The second one is proposed for correlation with visual color matching of fields subtending angle greater than 4°at the eye of the observer. A 10° visual field poses a diameter of approximately 90 mm at a viewing distance of 0.5 m. These color-matching functions are also given in CIE standard tables [8].

The connection between the angular subsense and the color effects can be also seen for example when observing optical phenomena in an atmosphere.

2.3. Light Sources

There is a large variety of sources that emit electromagnetic radiation and they are generally categorized according to the specific spectrum of the wavelengths generated by them. A vast majority of the visible light (and other frequencies out of the visible range) comes from the Sun. Then, there are many of artificial light sources, predominantly street lightings, tungsten, gas-discharge and fluorescent lamps, arc lamps, LEDs, lasers, or candle lights. The celestial bodies such as the Moon, stars, planets, Northern Lights (Aurora) or occasional shooting stars are the natural sources of light visible at night. The volcanoes and even biological sources like fireflies, jellyfish are natural light sources, too [4, 9].

The light source plays a very important role in colorimetry. The colors are mostly associated with objects which reflect or transmit the light emitting from the source of light.

Therefore, the color specifications relate to a particular light source. One needs to determine which source of light is the best to be used for a specific color matching application. The X, Y, Z tristimulus values or any colorimetric measures are substantially

meaningless for any reflecting or transmitting object, unless the light source is specified. So the proper choice and specification of the light source is essential in colorimetry [5].

There are usually various commonly available light sources listed in tables in literature with their brief description, usage, and application. Each of the sources has its specific temperature that is given in Kelvin scale. The lower the temperature is, the redder the source is. In Table 1, there are given the correlated color temperatures of selected commonly used light sources together with names and colors associated with them [5, 7].

Temperature	Source	Color
7500K	North - sky daylight (D75)	Moderate to deep blue
6500K	Average daylight (D65), LED with phosphor	Moderate blue
5000K, 5500K	Equal energy daylight (D50, D55), sunlight plus skylight	Cool white
4100K	Various fluorescent sources	Greenish
3500K, 3700K	Various fluorescent sources, LED	Orangish
3200K	Tungsten A	Red / Yellow
2865K	Illuminant A	Yellowish red
2300K, 2000K	Horizon, Sun light at sunset	Reddish

Tab. 1: Table of commonly used light sources correlated with temperature and color [4, 5, 7]

The color temperature can be explained by a blackbody radiation. A blackbody has no color and it absorbs the entire light incident on its surface. At the temperature of absolute zero (0K, -273°C) it looks perfectly black since it does not emit any light. Heated blackbody becomes luminous with a radiance and color dependent on a temperature. So it has a color of red at about 1000K, yellow at about 1500K, white at 4500K and bluish-white or moderate blue at the temperature of 6500K. The changes in blackbody´s color or spectral radiation are well described by blackbody radiation law – the Planck´s law [4].

A great variety of spectral distribution is provided by the commonly used light sources and standard illuminants. The colored objects undergo noticeable changes in color

appearance as the light source changes even in spite of adaptation of the visual system. Some pairs of the colors match under the one light source but may not necessarily match under another. Consequently, the CIE (International Commission on Illumination) standardized some illuminants and sources to simplify the complexity of not only color matching system. There is one difference established between illuminants and sources. Illuminants are defined in terms of spectral power distribution and sources are defined as physically feasible producers of radiant power (CIE, 2010) [5].

The only daylight illuminant which was actually measured is D65. This is the one with temperature around 6500K and bluish colored light. The temperature approximately corresponds to the temperature of the Sun – 6000K. The sources D75 and D50 (D55) were derived from the illuminant D65. D65 is mostly used as a primary light source in color matching applications and color measurement instrumentations [10].

Illuminant A is CIE standard tungsten illuminant linked to the historically most common artificial light source – tungsten filament lamp. The temperature is the only variable on which this source spectrum depends. It is primarily used in photographic industry but also commonly used in color matching applications [5, 8].

According to the experiment performed in terms of this bachelor thesis the illuminant D65 is considered as the most suitable for calculating the color-matching functions.

2.4. Color Spaces

A color model represents any color composed of a set of the primary colors. It is based on a mathematical description where one is able to describe a color by usually three values of color components. The set of colors is then called the color space. The basic composition of color models can be additive or subtractive. The best known color models are additive RGB for computer displays, subtractive CMYK usually for printing and XYZ as approximately reformulated tristimulus values of red, green and blue, similar to RGB.

CIE XYZ or CIE 1931 is one of the first mathematically defined color spaces and it is based on previous specification of CIE RGB color space, which came from series of experiments [5].

CIE XYZ color space is defined depending on sensitivity of the human eye (cones), where the color space is based on responses of three kinds of cone cells in the human eye with spectral sensitivity in short, middle and long wavelengths. In the human eye, there are also rods which operate at low level of illumination and have maximum sensitivity at lower wavelengths. The XYZ color space is proposed that Y means brightness and the color space is figured by x, y parameters – the chromaticity coordinates, calculated from X, Y, Z tristimulus values. The chromaticity coordinates of the spectral stimuli are ratios [10]:

$$x = \frac{X}{X+Y+Z}, \quad y = \frac{Y}{X+Y+Z}, \quad z = \frac{Z}{X+Y+Z}. \tag{2.1}$$

There is a normalization condition as follows $x + y + z = 1$ and the third component can always be deduced from the first two. The same equations apply to RGB tristimulus values calculations and normalization. Detailed calculation of tristimulus values is shown in Chapter 2.5.

The color space is shown by x, y chromaticity diagram in Figure 2.

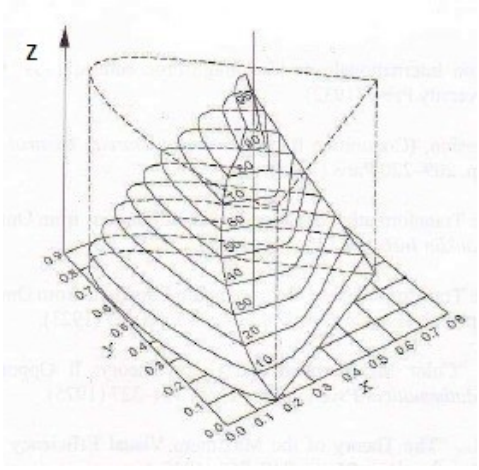

Fig. 2: CIE XYZ color space expressed by CIE x, y diagram [4].

The curve for Y tristimulus value indicates the human´s eye response to total power of the light source. The value of Y is called the luminance factor and has always the value of 100%. Other tristimulus values have been normalized [11]. The colors (X, Y, Z) are always constant in this color space contrary to RGB color space dependent on individual devices.

CIE XYZ color system is typically used to report the spectral response of measured sample and to interpret the color from measuring instruments. The sample is usually

measured by a colorimeter or a spectrophotometer. It is also possible to measure the color effects on ellipsometer as a function of incident light polarization.

RGB (red – green – blue) color space is based on additive color mixing with primary monochromatic colors which can be used in computer monitors, projectors or displays. The mixture is made of emitted light so it is not necessary to add an external light source in contrast to CMYK color space with subtractive mixing of colors. Human color space is sensitive the best to the mixtures of light of these red, green and blue primary colors and so the largest part of it can be captured right with this mixture of colors [12, 13]. It is possible to convert color-matching functions and tristimulus values from CIE RGB and CIE XYZ color spaces between each other (as described in Chapter 2.6).

CMYK represents subtractive color model which can be used in printing as well as in describing the printing process itself. CMYK refers to four main colors of inks used in color printing, which are Cyan, Magenta, Yellow and Key (black). The ink reduces the light that could be reflected from the surface and so induces the subtraction of brightness from white color. The background is usually white (paper) and a full combination of three colored inks is black. This is opposite operation to the RGB color model. Nevertheless, CMYK and RGB color spaces are both device dependent spaces and it is not so precisely convertible to each other because there exist some different colors which could not be achieved at one space in the chromaticity diagram (Fig. 3) [13]. When we look at the chromaticity diagram and highlight the RGB triangle boundaries, we encounter that RGB and CMYK color spaces do not match each other for some specific spaces – small ranges behind the borders of the triangle.

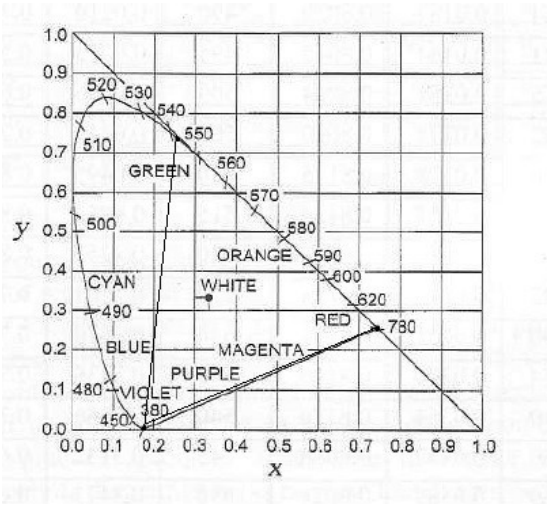

Fig. 3: Chromaticity x – y diagram for RGB and CMYK color space [4].

In the subtractive system white stands for the balanced reflection of all the hues in the light spectrum and the black stands for the absorption. So, in CMYK mixing the cyan, magenta and yellow color produces the forth black color and in RGB mixing the basic red, green and blue color produces white.

2.5. Calculation of Tristimulus Values and Chromaticity Coordinates

Mostly the XYZ color space and its values are taken as an example to describe the color calculations.

The mixture of CIE primary colors can be specified by three numbers X, Y and Z. CIE primaries are mathematically defined. The X, Y, Z tristimulus values specify lightness, hue and saturation of the color. It tells if the color is dark or light, which hue it has such as red, orange, yellow, green, blue or purple, hence different combinations of wavelengths; and how saturated the color is, what means for example red or pink, light blue or navy blue. The luminance factor Y is 100% for objects that do not absorb any light and 0% for those which absorb everything. Value of Y greater than 100% occurs for fluorescent objects [5].

Although, XYZ is similar to RGB system, they are not the same. X, Y, and Z numbers are mathematically created extrapolations of R, G, B values to avoid negative numbers in calculations [5, 14].

For correlations with visual color matching of field at the eye of the observer, it is recommended that colorimetric specifications of color stimuli should be based on the color-matching functions. Color-matching functions are monochromatic radiations for a set of reference stimuli X, Y, Z required to match each wavelength of the equi-energy spectrum, where equi-energy spectrum is a spectrum of radiation. Its spectral concentration of radiometric quantity as a function of wavelength is constant throughout the visible part of the electromagnetic spectrum. The color-matching functions are commonly used in obtaining the tristimulus values of the specific color space [5, 7]. The values of the color-matching functions $\bar{x}(\lambda), \bar{y}(\lambda), \bar{z}(\lambda)$ or $\bar{r}(\lambda), \bar{g}(\lambda), \bar{b}(\lambda)$ are given as the normalized tabulated values from the wavelength 360 nm to 830 nm [4, 8] at 1 nm intervals (Fig. 4).

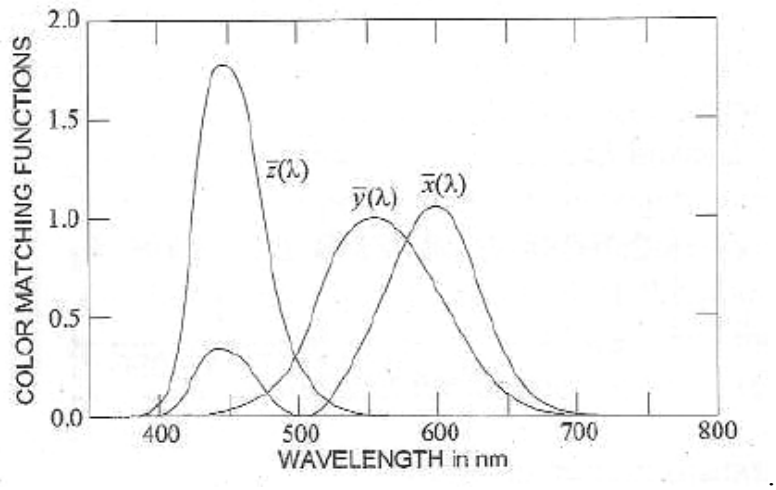

Fig. 4: CIE XYZ - the $\bar{x}(\lambda), \bar{y}(\lambda), \bar{z}(\lambda)$ color-matching functions [4].

To calculate the tristimulus values the measured or calculated spectra with wavelength values are also needed. The interval of measured wavelength is 1 nm for visible spectrum while the interval for tabulated coordinates is 5 nm. Due to the different intervals of these wavelengths the linear interpolation with tabulated coordinates and measured values needs to be performed. In measurements with no significant errors the data from another standardized table with 5 nm intervals can be used. Then the interval of wavelength and the interval of color-matching functions correspond to each other.

The reference stimuli X, Y, Z or R, G, B were chosen for reasons of convenience in colorimetric computations. The color-matching functions are commonly used to obtain the tristimulus values of color stimuli [7].

Then, one can calculate the tristimulus values from the color-macthing functions with the use of the following equations

$$X = \int_0^{\infty} \bar{x}(\lambda) \cdot R\,(\lambda) d\lambda = \sum_{i=1}^{N} x_i \cdot R_i \cdot \Delta\lambda, \tag{2.2}$$

$$Y = \int_0^{\infty} \bar{y}(\lambda) \cdot R\,(\lambda) d\lambda = \sum_{i=1}^{N} y_i \cdot R_i \cdot \Delta\lambda, \tag{2.3}$$

$$Z = \int_0^{\infty} \bar{z}(\lambda) \cdot R\,(\lambda) d\lambda = \sum_{i=1}^{N} z_i \cdot R_i \cdot \Delta\lambda, \tag{2.4}$$

where $R(\lambda)$ are the intensity values from spectra and λ is the wavelength. $\Delta\lambda$ corresponds to the difference between two nearby wavelengths. x_i, y_i, z_i values are the interpolated tristimulus values [8]. The same equations apply to RGB tristimulus values.

Then, the chromaticity coordinates can be obtained from the calculated tristimulus values. The Y tristimulus value correlate with brightness but the others, X and Z do not correlate with anything. Therefore it is important to find such correlates using other method derived from the tristimulus values to find those missing perceptual attributes. Important color attributes refer to the relative amounts of the tristimulus values [5].

The chromaticity coordinates are then calculated from the spectral power distribution of light and the CIE trisstimulus values, as shown in equation (2.4). They are always labeled by lower-case letters and they represent the relative amounts of tristimulus values. Chromaticity coordinates specifiy the hue and saturation of the color, but not its lightness.

2.6. Transformation of Tristimulus Values and Chromaticity Coordinates

The individual coordinates or tristimulus values of the specific color spaces can be easily transformed one into another using given matrices and the coefficients for the given light source (e.g. illuminant D65).

There are plenty of converting formulas, each corresponding to a different type of illuminant or the light source, various types of the observer or different types of typical white points in the chromaticity diagram. For calculating standard CIE color-matching functions defining the color matching properties of the CIE 1931 Standard Colorimetric Observer (2° observer – see chapter 2.2.1.), the matrix is taken from reference [5], rather than from internet sources for several Adobe, Hp or other variations.

To avoid negative numbers in color specifications, the tristimulus values R, G, B should be replaced by X, Y, Z tristimulus values, which are obtained by means of the equations [5]:

$$X = 0.49R + 0.31G + 0.20B, \tag{2.5}$$

$$Y = 0.17697R + 0.81240G + 0.01063B, \tag{2.6}$$

$$Z = 0.00R + 0.01G + 0.99B. \tag{2.7}$$

So we use matrix:

$$\begin{bmatrix} X \\ Y \\ Z \end{bmatrix} = \begin{bmatrix} 0.49 & 0.31 & 0.20 \\ 0.17697 & 0.81240 & 0.01063 \\ 0.00 & 0.01 & 0.99 \end{bmatrix} \cdot \begin{bmatrix} R \\ G \\ B \end{bmatrix} \tag{2.8}$$

The numbers were carefully chosen by CIE. To calculate RGB tristimulus values from XYZ, we must use the inverse matrix to that one shown in equation (2.11).

Color-matching functions can be calculated from each other, too. For example calculating color-matching functions $\bar{x}(\lambda), \bar{y}(\lambda), \bar{z}(\lambda)$ from $\bar{r}(\lambda), \bar{g}(\lambda), \bar{b}(\lambda)$ by the same matrix as the tristimulus values [5, 9].

There is also a matrix conversion between the RGB and CMYK color space. Exactly, there must be first the CMY color space derived from RGB and later then it can be used for color printing. The problem comes in with the ink imperfections so the CMY does not reproduce black color well. Instead of it, the better known model of CMYK is used in practice. The conversion is given [12]:

$$\begin{bmatrix} C' \\ M' \\ Y' \end{bmatrix} = \begin{bmatrix} 1-R \\ 1-G \\ 1-B \end{bmatrix}, \quad \begin{bmatrix} K \\ C \\ M \\ Y \end{bmatrix} = \begin{bmatrix} \min(C', M', Y') \\ \frac{C'-K}{1-K} \\ \frac{M'-K}{1-K} \\ \frac{Y'-K}{1-K} \end{bmatrix} \tag{2.9}$$

3. COLOR EFFECTS IN ATMOSPHERIC OPTICS

As we can see, the colors can be found everywhere. The main architect of the whole range of colors is nature. It is not just colored itself, but on certain occasions and under suitable conditions it can create a precious show by different color effects, that are not only interesting and beautiful to look at, but also scientific from the physical point of view.

The color effects are mostly based on three basic optical phenomena such as reflection, refraction and diffraction. Their origin is related to water droplets, ice or dust particles in the atmosphere in most of the cases, so the conditions for observing them are better in colder places, for example in the north of the Earth. The polarization of light plays the role

in color effects, too. The manner in which the polarization occurs depends strongly on the path the light has taken. The amount of polarized light is at least as large as amount of color in nature. Still, the differences in polarization in the scenery are barely visible by the naked eye compared to colors in nature.

Among the color effects resulting from the atmospheric physics are rainbow, halos, mother-of-pearl clouds, noctilucent clouds or twilight phenomena, but also northern lights (auroras) or flashlights. Some of them are very special due to their wealth of colors. For this thesis, only few of them are chosen and described because of thre extensiveness of the topic.

3.1. Main Optical Principles in Atmospheric Optics

3.1.1. Reflection and Refraction

Reflection and refraction come under geometrical optics where the light propagates in the form of rays, as the trajectories of photons. If the light beam is incident on an interface between two media with different optical characteristics, the light is partially reflected from the interface and partially refracted to the second medium. Reflection does not cause any color effect, the colors originate by refraction.

The light travels throughout the different media like water droplets, ice crystals or some other particles in the atmosphere. The speed of light in a given materials is related to index of refraction, *n*, which is defined as the ratio of the speed of light in a vacuum, *c,* to the speed of light in the medium *v*. Mathematically, it is then $n = c/v$. The speed changes while traveling through different media and also with the wavelength. The angle of transmission of light into the second medium is related to the angle of incidence by Snell´s law [3]:

$$n_1 sin\alpha_1 = n_2 sin\alpha_2;\ \frac{sin\alpha_1}{sin\alpha_2} = \frac{v_1}{v_2} = \frac{n_2}{n_1} \qquad (3.1.)$$

3.1.2. Interference and Diffraction

Interference and diffraction are both phenomena of wave optics based on the superposition of two or more coherent waves.

The result of the interference depends on phase difference of the waves. Phase difference is composed partly of difference of optical trajectories and partly of the phase change upon reflection. According to reciprocal phase of the waves, the constructive or destructive interference may happen. If one wave meets another wave of the same frequency at the same spot, the constructive interference turns up. Then, the total wave amplitude is the sum of the individual amplitudes. The destructive interference occurs if one wave meets another wave of opposite phase. Then the total wave amplitude is equal to the difference in the individual amplitudes of the waves [15, 16]. Interference is crucial effect in measuring the color effects by reflection from thin films.

In diffraction, the light propagates in a form of waves and their surface is perpendicular to light rays. Every spatial limitation of light waves (planar of spherical) with an obstacle leads to a flexion of the waves. The light propagates beyond and around the obstacle after the incidence of the wave on the edge of the obstacle. The diffraction occurs in iridescent clouds, coronas or glorioles where the particles are small with similar size and they individually scatter light. The size of a particle is not much larger than the wavelength of the visible light. The diffracted spectrum disperses into rainbow colors and they are dependent on the wavelength, the longer wavelength, the more waves diffract.

3.2. Rainbow

A rainbow is the most famous optical phenomenon in the sky. It has a shape of a band with the full spectral range of colors from blue color inside to red outside (primary rainbow). It is formed when the Sun light shines directly on water droplets. It is possible to see the colored band at about 138° from the Sun, usually 42° from the anti-solar point (with the Sun at our back). Rainbows can be seen for example in rainy weather, but also near waterfalls, fountains, showers or geysers. The secondary rainbow can appear at about 8° outside the primary rainbow and it has reversed color order. The colors of the rainbow correspond to the colors of which the source of light is composed [17].

The principle of rainbow formation is in refraction and inner reflection of incident light in water droplets (Fig. 5).

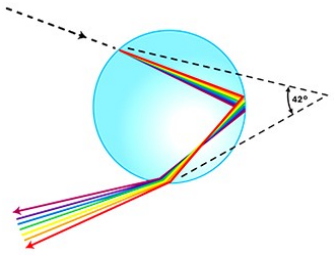

Fig. 5: The light path in the water droplet forming the primary rainbow [18].

Because of different physical properties of water droplets and ice crystals, each type of particles create different optical phenomenon.

3.3. Halos

Halos are optical phenomena which appear on the sky around the Sun and the Moon. It has a shape of a circle. The condition for its appearance is a presence of ice crystals in the atmosphere. On the ice crystals, the refraction of light occurs. It is visible at altitudes above 6 km, in high clouds but it can occur also in cold ground layer of the atmosphere. Halos can also be observed in falling snow crystals, freezing fog, on snow covers and on surfaces covered with hoar-frost. Depending on whether the light is reflected from small ice crystals or it passes through them and refracts, the appearance of halos is either whitish or with iridescent tint [19].

Halos are caused by refraction in ice crystals with the shape of hexagonal columns and plates, where plates are often horizontally aligned (sun dogs). Special symmetrical case gives lowest deviation angle of 22°. A sharp edge on one side of a halo is oriented towards the lower deviation angle. Like in a prism, the color depends on the angle of refraction [20].

3.3.1. Types of Halo

There is a great variety of types of halos, some of them are common and others appear only once every few years. The most important and frequently occurring halos can be divided roughly into three groups.

The first group are phenomena with a radius of 22° from the Sun – small halos. They have a form of a bright circle around the Sun or very bright spots in either side of the Sun, the perihelia. Red color is nearest to the Sun and usually very conspicuous. Orange and yellow colors are still visible but the other colors are paler.

In the second group are weaker but more colorful halos of the same character and with the same sequence of colors at about 46° from the Sun – the big halo. Its plenty of colors may exceed that of rainbows [17]. It occurs rarely and it originates by double refraction on randomly oriented hexagonal ice crystals. The Sun ray enters the bottom of the crystal and goes out from the side wall. Hence, the path of the rays in the ice crystals is different from more frequent small 22° halo effect [21]. Even under a considerably high concentration of ice crystals in the air, when the small halo is visible simultaneously, the big halo is considerably weaker [19].

The third group includes uncolored spots (appearing white) and bands in several places in the sky – reflection halos. By moonlight our eyes are almost insensitive to colors and almost all halos seem to be colorless except of a perihelion which is the only bright one and still displays colors. Perihelia, usually called the Sun dogs, occur at 22° at either side of the Sun [19]. Basic types of halos are shown in Figure 6.

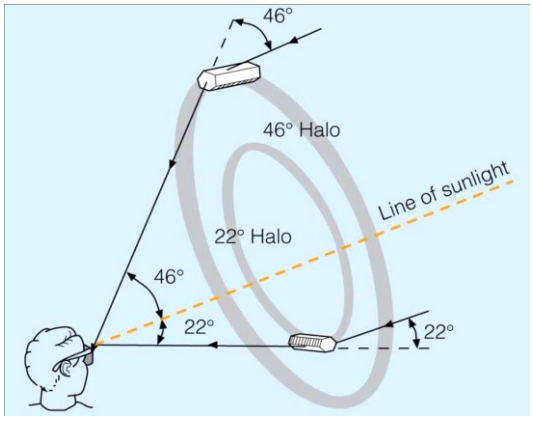

Fig. 6: Halo effects on ice particles. Double refraction is bending the sun ray by 22° from its original direction and creating the circle of light visible at a distance of 22 degrees from the Sun [3, 21].

All the halo angles can be calculated by Snell´s law (2.1), similarly to procedure shown in Figure 7. To simplify the calculation, we assume rays perpendicular to the refraction edge. The angle of incidence is $\varphi_1$and the refracted angle is φ_1' and similarly for φ_2 and φ_2'. The δ angle is the deviation of the ray, n is the refractive index of the ice.

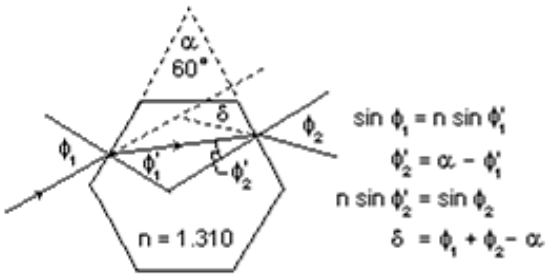

Fig. 7: The light trace in hexagonal ice crystal – calculation of angles by the Snell´s law [22].

3.4. Iridescent Clouds, Mother-of-pearl Clouds and Noctilucent Clouds

Iridescent clouds can vary by different colors. They are refraction and diffraction phenomenon. There are different shapes of clouds which can display color bands, predominantly green or red, which occurs at a different distances from the Sun. The colors are formed in the area where water droplets are nearly the same size and the distance between the two rings of the same color is determined by the size of the cloud droplets [20, 21].

When the light bends around a water droplet, the diffraction occurs. The extent of bending depends on the wavelength. Each wavelength is diffracted in a different ratio. Optically thin cloud or edge of the cloud shines more. On the thick body of the cloud, the multiple scattering prevails and so the colors disappear [23].

Mother-of-pearl cloud is a type of a polar stratospheric cloud (PSC). It can be also called nacreous cloud due to its color which can be compared with the color of the inner layer of the shell of some mollusks or seashells [24]. Mother-of-pearl clouds are visible at higher latitudes when the Sun is below the horizon and the Earth surface and lower layers of the atmosphere are already in the shadow. It is a rare type of a cloud appearing in heights around 20 – 30 km in the stratosphere. Normal clouds are usually in latitudes around 10 to 12 km [25]. Small highly supercooled water droplets are a basis for the

significant iridescence of these clouds. Their pearly brightness is reflected expressively on the twilight sky, when they are illuminated by the last sun rays after the sunset or sunrise. The shine of these clouds is made by diffraction in water droplets or ice crystals which scatter light [24].

Noctilucent clouds belong to a group of polar mesospheric clouds (PMC). They are visible after sunset and they are formed at extreme heights, at about 80 km in the mesopause. The best places to observe these clouds are in the polar region where the mesopause is coldest (< -120°C), in summer months. They have silvery white color and appear always in the direction of the sunset when the sky is very clear. The silky luminous clouds are visualized towards the dark sky. They are lit by the Sun for a long time after the sunset because of their height. It is a relatively rare phenomenon [3, 5].

All these types of clouds are shown in Figure 8.

Fig. 8: Iridescent clouds, mother-of-pearl clouds and noctilucent clouds

3.5. Corona, Gloriole

A corona is mostly related to the Moon. The coronas can reflect whitish or colorful homocentric rings around the light source when the light shines through the layer of water droplets in the clouds. A position of the color rings depends on the wavelength and diameter of the droplets. Colors are sorted similarly to a rainbow [26]. It is a diffraction phenomenon and the angular diameter of the ring around the light source is inversely proportional to the diameter of the cloud particles.

A gloriole could be considered as the most remarkable effect in the atmospheric optics. It looks similar to a corona but it shines with significantly less intensity. It poses some kind of a halo visible around the shadow of the observer´s head. It is in the form of colorful rings around the shadow which is placed on the layer of clouds or fog [5].

These optical phenomena are in general caused by a combination of reflection, refraction and diffraction. The light encountering a cloud droplet is mostly bent almost 180° backwards to the observer (Fig. 9) [26].

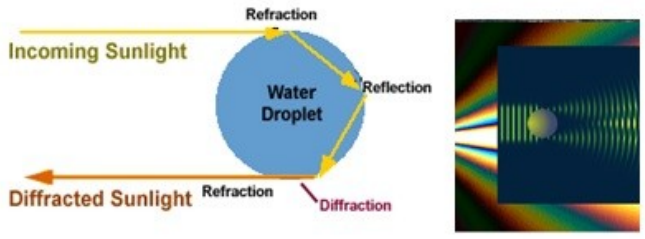

a) b)

Fig. 9: a) The origin of optical phenomena in a water droplet caused by refraction, reflection and diffraction – Corona, Gloriole [26], b) The diffracted spectrum caused by a small particle [20].

3.6. Aurora – Northern Lights

An Aurora is a phenomenon mostly seen near the northern or southern poles. The Aurora observed in the northern part is called the Aurora Borealis while the one observed in the southern part is the Aurora Australis. They are referred to as northern lights and southern lights.

This phenomenon is caused by fast-moving electrons from solar wind colliding with and thereby exciting electrons of molecules in the atmosphere at about 100 - 300 km altitude range. The excited electrons emit photons whose wavelength corresponds to the excitation energy of an atom.

An aurora activity is directly related to the activity of the Sun, the source of the energetic electrons. Solar wind interferes with the Earth´s magnetic field, causing the magnetic field of night-sided region of the Earth stretched like a long tail. The place with the highest probability of occurrence of an aurora is called the aurora oval. It could be described as an annual ring around each geomagnetic pole of the Earth [24], where the Earth´s magnetosphere does not deviate the electrons from the solar wind by Lorentz force.

Colorful auroras originate due to magnetic substorms, a local disturbance in the magnetic field acting in the auroral zone. They can be regularly observed in auroral regions

from the ground, space stations or satellites [27]. The pre-requisites for an aurora are the atmosphere, the charged particles which hit the atmosphere, the magnetic field to guide the particles to the atmosphere, the energy source (the Sun) to give the particles enough energy to generate aurora and the power transfer system to carry energy from the source to the charged particles - Solar wind and the magnetosphere [28].

An aurora´s description fits the particle physics better but from optical point of view, one can see auroras in various colors and their combinations corresponding to different wavelengths and altitudes. The highest part of the aurora is red, the middle part is green and the lowest part has usually pink or purplish color. When the light transits from green to red, the changes of light are sometimes visible with orange or yellow color due to the mixture of green and red colors.

Probably the most frequently seen color in auroras is green which corresponds to the spectral line with the wavelength 557.7 nm and it is caused by the atomic oxygen emission. This aurora occurs at an altitude of 100 – 200 km [24]. The second one is red with the wavelength of 630 nm. Red upper regions with the green color dominant in the lower regions are often observed in the form of the band-shaped auroras. Red color due to the first positive bands of molecular nitrogen appears at very low heights (about 70 km), mostly as the margin along the lower border of the band that is dominantly green above. The red auroras originate from majority of the red atomic oxygen lines [27]. It is more possible to see this spectral line (630 nm) in the upper borders of auroral arcs, at high altitudes (> 300 km). Thay can be usually observed only after largest coronal mass ejections on the Sun [24]. The green color in oxygen emissions prevails due to a shorter time of the atom needed to return to the ground state and a higher density of the atmospheric gas at lower altitudes (Fig. 10) [29]. The white color is usually associated with low levels of luminance and scotopic (night) vision. Seldom, the appearance of white or yellow may arise from appropriate proportions of green (557 nm) and red (630 nm) color formed from collisions with atomic oxygen and blue (391 nm, 427 nm) from ionized molecular nitrogen bands. The blue color is being dominant during or after the very active displays. Then, the purple color appears as a mixture of red and blue. These colors are more noticeable in the upper regions of the aurora and they intensify when the regions are sunlit [27].

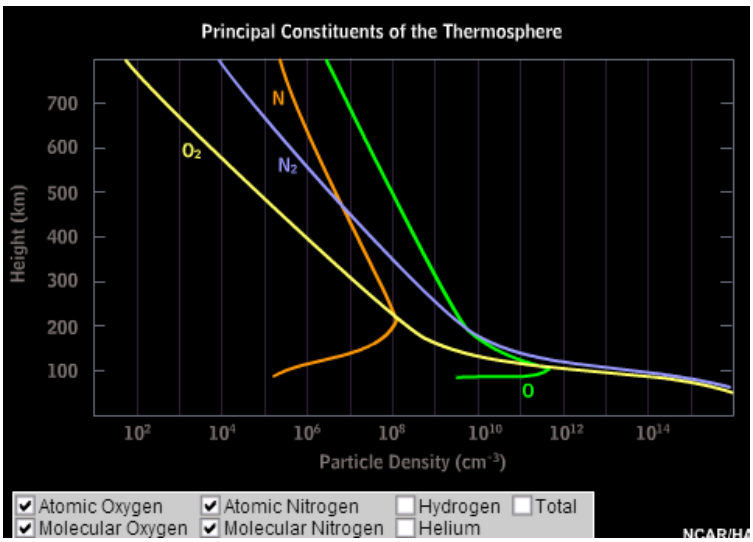

Fig. 10: Density of the gas depending on the altitude [29].

The view of all colors, altitudes and relevant gases is rendered in figure below (Fig. 11). We can also anticipate some connection between aurora´s spectrum and the electromagnetic spectrum created by dispersion of light.

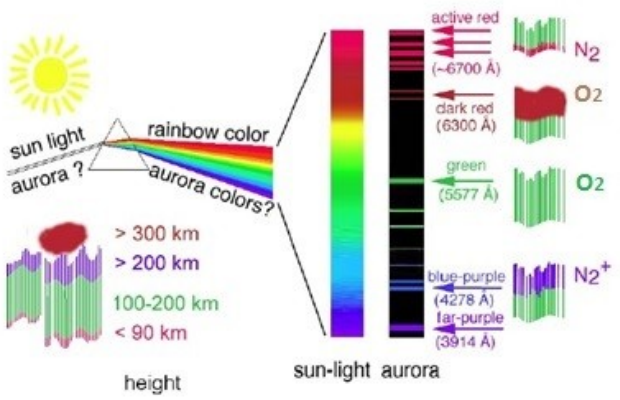

Fig. 11: Spectral colors in aurora, altitudes of their appearance and particular ionized gases. The aurora´s spectrum compared to rainbow color spectrum caused by dispersion [30].

The spectroscopy of the luminous aurora is based on a grating spectrograph, a high speed camera for recording the image, a TV system, a photomultiplier, photocell or infrared converter. The Fabry-Perot monochromator or an interference filter may be used to observe a selected spectral line [30]. Typical auroral spectral lines of all gases are shown in Figure 12.

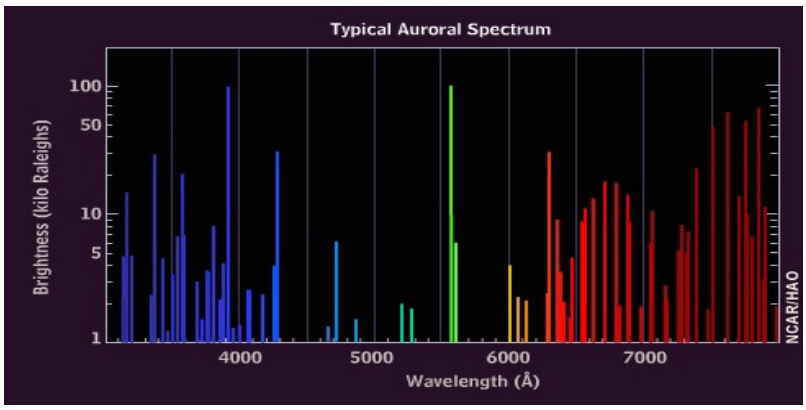

Fig. 12: Typical auroral spectrum – intensity dependent of the wavelength [31]

The recent developments in optical instrumentation have helped to improve a spectral resolution significantly. Optical measurements provide higher resolution compared to other types of ground-based devices used in auroral studies. The improvements have given rise to advanced techniques of analysis or modeling of the aurora which helps scientists to examine its physical and optical principles together with the essence of auroral light formation [32].

3.6.1. Models of Colors of Aurora

Using the spectral lines gases inatmosphere – the intensity spectrum and the known wavelengths of each color corresponding to transmissions in gasses, it may be possible to calculate the color coordinates.

The values of wavelengths and relative intensities are taken from the Ref. [33] and compared to the spectrum shown in Figure 10. The trichromatic coordinates are calculated as shown in equation (2.8), and each of them is multiplied by the gradually changing contribution of the gasses. The modeled is then a graph with the pure elements and their colors in chromaticity diagram (Fig. 13).

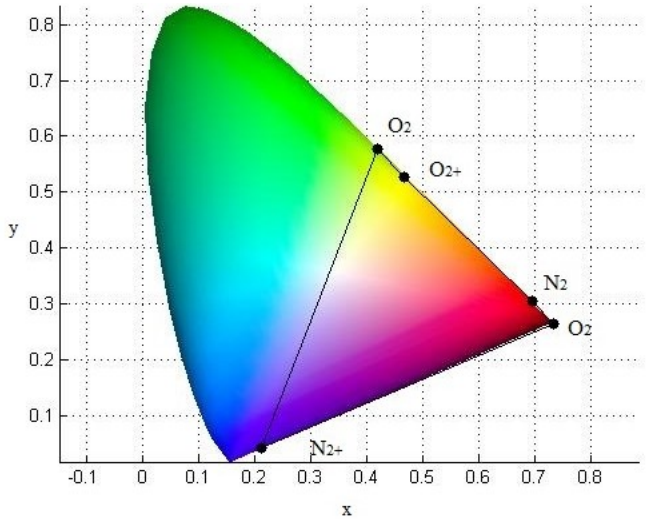

Fig. 13: Modeled colors of pure gas elements in Aurora

Next modeled dependence shows the changes of colors of the aurora during the solar wind transiting throughout the layers of different gasses and different altitudes in the atmosphere. There is chosen the color transition between nitrogen atoms at low altitudes and oxygen atoms in altitudes about 200 km. The values of the concentrations dependent on height in the atmosphere were taken from Ref. [34]. Model represents the x, y chromaticity diagram and the r, g, b column with continuously changing color from blue or purplish to green (Fig. 14).

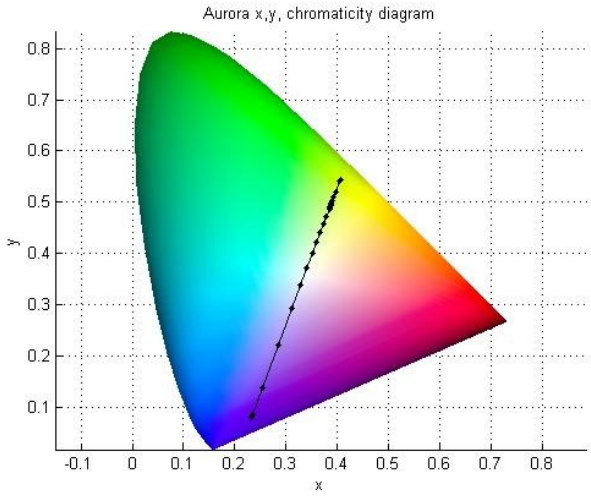

Fig. 14: Modeled color transition between the secondary nitrogen atoms to the oxygen atoms; colors in x, y chromaticity diagram.

There are also r, g, b, color coordinates for the transition mentioned above shown in the Figure 15. According to the altitudes of the gasses the color is changing from blue in the lower altitudes to greenish in higher altitudes.

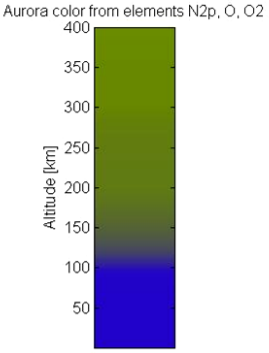

Fig. 15: Calculated r, g, b colors of the aurora transition (secondary nitrogen to oxygen), dependence on the height

The color functions of intensity of the aurora and its height is plotted in Figure 16.

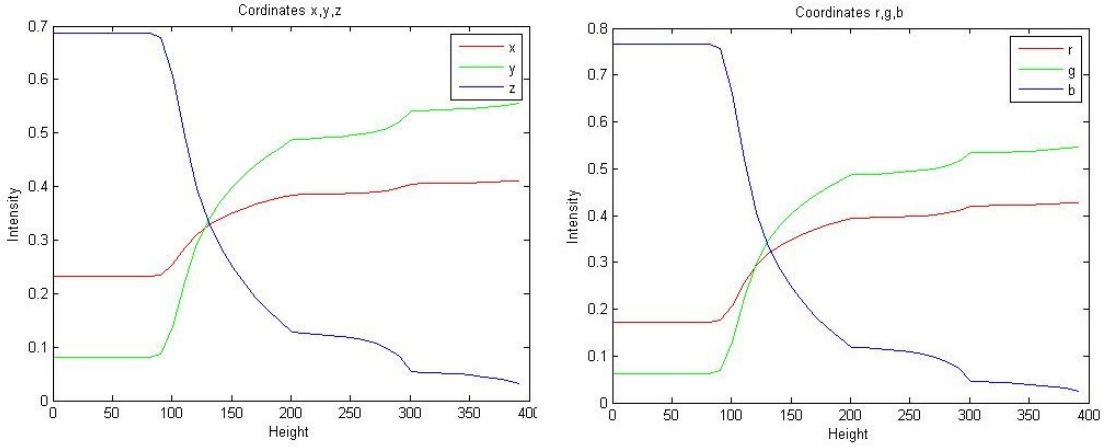

Fig. 16: The x, y, z and r, g, b trichromatic coordinates of the aurora N_2^+ to O_2 transition

4. COLOR EFFECTS BY REFLECTION FROM THIN FILMS

Color effects by reflection from thin films depend on optical constants of the material, propagation of the light in the thin film given by matrix formalism, reflection coefficients and total intensity spectra depending on the wavelength. The thickness of the thin film plays an important role, too. The use of measurement method depends on the polarization

of light and a sample. For measuring color effects on SiO_2 on Si thin films, the ellipsometric method was used.

The illuminant D65 is considered as the most suitable for calculating the color-matching functions.

4.1. Thin Films

Today, we are able to prepare and characterize thin films, to describe their structure and behavior and to model their optical, electrical, magnetic and mechanical properties.

Initially, the interest of science in thin films was focused on the optical applications, where the main charge was to measure film thickness and optical properties. Nowadays, the usage of thin films is spread in wide field of applications and they are used in many industries. The reason why thin films are so much in use is that scientists were able to discover their special properties resulting from their structure and dimensions. Thin films are one dimensional nanostructures, it means they have one proportion less than 100 nm. It is something between bulk materials and nanostructures, thus some physical properties of thin films are analogous to those of nanostructures. It has also bigger surface-to-volume ratio than bulk materials.

To characterize thin films we use in-situ and ex-situ characterization methods, which include optical methods (spectroscopy, ellipsometry) and weight methods, structural characterization and chemical characterization techniques [35]. For our purpose, to measure reflection of the thin films to observe color effects and calculate the coordinates from their measured or modeled optical spectra, the spectroscopic ellipsometry is used.

4.2. Calculating the Spectra

A variety of approaches have been used to calculate optical response from thin films and multilayers. The main step is to set up Maxwell´s equations and apply appropriate boundary conditions to obtain a solution [36]. The boundary conditions for electromagnetic waves require that the parallel components of the electric field **E** and the magnetic field **H** to the interface remain unchanged.

First, a suitable model for the dielectric function containing an information about the material should be found. Then, the optical constants may be calculated. This first step deals with the description of material parameters like refractive index, absorption coefficient, or the complex dielectric constant.

Secondly, the Maxwell´s and Helmholtz equations have to be solved in a system with the given material parameters and geometry. Then we obtain electric or magnetic fields which may be converted to light intensities and the light intensities are compared with experimental data. Changing the systems geometry will change the intensities obtained at the output, although the material might be the same.

Practically, there is more often a reverse process where the spectra have been measured and the optical constants have to be calculated. This reverse search and data fitting is more complicated in the thin film spectroscopy than the forward search [37].

4.3. Measuring the Optical Spectra – Spectroscopic Ellipsometry, Polarimetry

The spectroscopic ellipsometry is an optical measurement technique which uses the polarized light to characterize optical properties of materials, either by reflection or transmission of light. It is usually used to determine a thickness of a thin film and optical constants. The name Ellipsometry has its origin in polarized light that becomes elliptically polarized upon light reflection [38].

4.3.1. Polarization of Light

The polarization of light represents a strong basis for all ellipsometric measurements. It can be understood as a behavior of the wave´s electric field in space and time. The electric fields of light are oriented in specific directions.

If the oscillating direction of the light waves is random, we talk about unpolarized light. According to the phase difference between the light waves, the polarization changes from linear to circular polarization [38]. The completely polarized light means that the relative phase between the different components of the electromagnetic field along two orthogonal directions remains constant. When the waves are 90° out of phase and have

equal amplitude, the light is circularly polarized. The general elliptical polarization is a combination of orthogonal waves of an arbitrary amplitude and phase (Fig. 17).

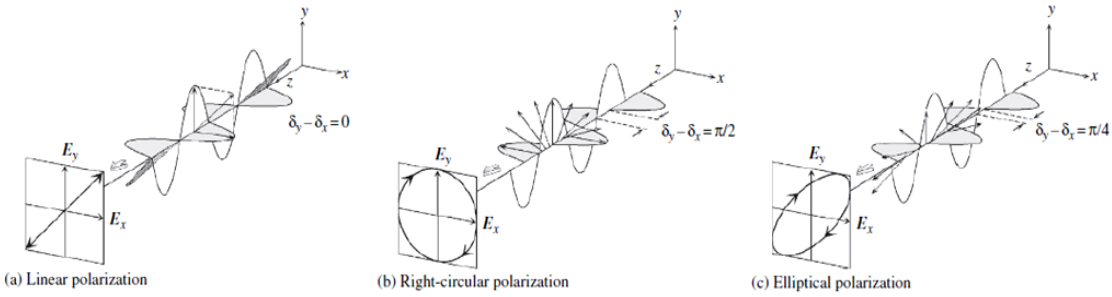

Fig. 17: Representations of (a) linear polarization, (b) circular polarization and (c) elliptical polarization [38].

To get control of principles of ellipsometric measurement it is important to comprehend the Jones formalism and Stokes – Mueller formalism to be able to describe the polarization of light mathematically.

4.3.2. Ellipsometry –Jones and Stokes-Mueller Formalism

The ellipsometry measures the change in polarized light upon reflection or transmission throughout a sample. The light beam remains completely polarized during the classical ellipsometric measurement. Therefore, it is essential to use a more general technique for a correct measurement and interpretation of the physical properties of partially polarized light. The technique is called the Mueller Ellipsometry or Mueller Matrix Polarimetry. Thanks to Mueller Matrix Polarimetry one is able to characterize anisotropic or depolarizing samples that are interesting for scientific research [39].

Data representing the polarization change are the ellipsometric angles Ψ and Δ which are amplitude upon reflection and the difference in phase shift – ratio between s- and p - polarized light. The spectra are measured by changing the wavelength of the incident light. Spectroscopic ellipsometry measurements are carried out in the UV, visible or infrared region [38].

In the polarimetry, the measured data except of ellipsometric angles are depolarization of the material, intensity – mean reflectivity of unpolarized light, error Ψ, error Δ and error of depolarization as a function of the wavelength λ, the angle of incidence and Mueller

matrix components. The benefit of the ellipsometric measurement is the direct interpretation of real and also an imaginary component of the complex dielectric function through the ellipsometric angles. The dielectric function relates to the refractive index *n* and the extinction coefficient *k* as follows [40]

$$\varepsilon = (n + ik)^2. \tag{4.1.}$$

The complex dielectric function is essential in examination of material´s electronic structure.

As the ellipsometric measurements are generally performed in reflection or transmission configurations, it is ordinary to choose the components of s- and p-polarization as reference for x, y coordinates. Jones vector is then [39]

$$J = \begin{pmatrix} E_x \\ E_y \end{pmatrix} = \begin{pmatrix} E_p \\ E_s \end{pmatrix}, \begin{pmatrix} {E_p}^{out} \\ {E_s}^{out} \end{pmatrix} = \begin{pmatrix} J_{pp} & J_{ps} \\ J_{sp} & J_{ss} \end{pmatrix} \begin{pmatrix} {E_p}^{in} \\ {E_p}^{in} \end{pmatrix}. \tag{4.2}$$

The Jones matrix is diagonal for isotropic samples. It consists of the Fresnel reflection or transmission coefficients in the polarization parallel (r_p) and perpendicular (r_s) to the plane of incidence [39, 41]:

$$J = \begin{pmatrix} {E_x}^{out} \\ {E_y}^{out} \end{pmatrix} = \begin{pmatrix} r_p & 0 \\ 0 & r_s \end{pmatrix} \begin{pmatrix} {E_x}^{in} \\ {E_y}^{in} \end{pmatrix} \tag{4.3}$$

The same stands for the transmission coefficients (t_p and t_s). The elipsometric angles Ψ and Δ are defined by the ratio [39, 41]: $\rho = \frac{r_p}{r_s} = \tan\psi e^{i\Delta}$, (4.4.)

where

$$r_s = \frac{n_1 cos\alpha_1 - n_2 cos\alpha_2}{n_1 cos\alpha_1 + n_2 cos\alpha_2}, \qquad r_p = \frac{n_2 cos\alpha_1 - n_1 cos\alpha_2}{n_1 cos\alpha_2 + n_2 cos\alpha_1} \tag{4.5}$$

are the Fresnel reflection coefficients.

The Jones vector is used only for totally polarized light. To be able to describe partial polarization of depolarization of the sample, one has to determine the Stokes – Mueller matrix. The Stokes vector includes a description of totally polarized, partially polarized, and also non-polarized light. The Stokes vector is determined as follows [42]

$$S = \begin{bmatrix} I \\ Q \\ U \\ V \end{bmatrix} = \begin{bmatrix} I_p + I_s \\ I_p - I_s \\ I_{45^\circ} - I_{-45^\circ} \\ I_L - I_R \end{bmatrix}, \tag{4.6}$$

where I is the total intensity, Q is the difference between linear polarizations along x and y axes, U is the difference between the linear polarizations in directions $\pm 45^\circ$ and V is the difference between the left-handed and right-handed circular polarization. The degree of the polarization is defined by an equation $\rho_s = \frac{\sqrt{Q^2+U^2+V^2}}{I}$, where for totally depolarized light is $\rho_s = 0$ and for totally polarized light $\rho_s = 1$ [39, 42].

The transformation of the Stokes vector by a 4 x 4 matrix representation is referred to as the Mueller matrix. To obtain an information about the interaction of any other than totally polarized light and the sample, the Stokes vector is transformed by the well-known Mueller matrix **M** [39, 42]:

$$S^{out} = \begin{bmatrix} I \\ Q \\ U \\ V \end{bmatrix}^{out} = \boldsymbol{M} S^{in} = \begin{bmatrix} M_{11} & M_{12} & M_{13} & M_{14} \\ M_{21} & M_{22} & M_{23} & M_{24} \\ M_{31} & M_{31} & M_{33} & M_{34} \\ M_{41} & M_{42} & M_{43} & M_{44} \end{bmatrix} \cdot \begin{bmatrix} I \\ Q \\ U \\ V \end{bmatrix}^{out}. \tag{4.7}$$

Measuring the whole Mueller matrices gives a complete information about the interaction of light with the samples including complex anisotropy or depolarization effects. The Mueller matrix polarimetry is the most suitable technique able to characterize a response of any sample under any conditions [39].

In terms of the ellipsometric angles Ψ and Δ, the Mueller matrix of an isotropic, nondepolarzing sample is rewritten as follows [39]

$$M(\Psi, \Delta) = \begin{bmatrix} 1 & -\cos(2\Psi) & 0 & 0 \\ -\cos(2\Psi) & 1 & 0 & 0 \\ 0 & 0 & \sin(2\Psi)cos\Delta & \sin(2\Psi)sin\Delta \\ 0 & 0 & -\sin(2\Psi)sin\Delta & \sin(2\Psi)cos\Delta \end{bmatrix} \tag{4.8}$$

4.4. Ellipsometric Measurement

The basis of the ellipsometric measurement is an ellipsometer which usually combines high accuracy and precission together with wide spectral range from UV to near infrared. The ellipsometer consists of several parts such as a light source, a polarization generator

and a polarization sensitive detector realized for example by a rotating analyzer containing a rotating polarizer, a rotating compensator, or a phase modulator. It is possible to measure all 16 elements of the Mueller matrix [43].

For measurements performed for this thesis, the VASE ellipsometer RC2 from J. A. Woollam Co., Inc. Corporation is used. It comprises a dual rotating compensator and enables the complete Mueller matrix characterization. A software for enquiring and exporting all the data from the measurements is called the CompleteEase and is made by the same company as the ellipsometer mentioned above.

The schematic illustration of the ellipsometric measurement is shown in Figure 18.

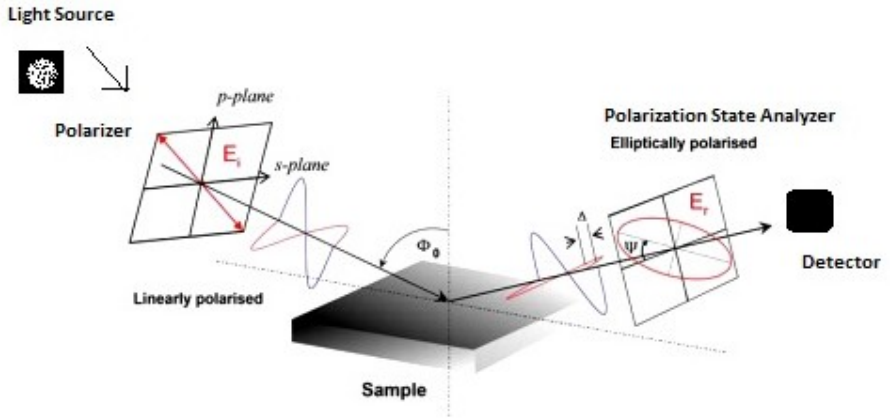

Fig. 18: Typical configuration of an ellipsometric measurement. Linearly polarized light is reflected from the surface at the angle of 45◦ and the polarization change is measured in order to determine the response of the measured sample [41, 43].

4.5. Experimental Part

The modeled spectrum was calculated from the tabulated optical constants of the SiO_2 on Silicon thin film using MATLAB software with regards to the matrix formalism of the thin films.

Thin films of 10 nm, 25 nm, 60 nm and 1000 nm thickness were measured. In a thick film the light interferes and creates more visible color effects than in a thinner medium. Therefore, 1000 nm thick SiO_2 on Silicon film is the most suitable for study in this thesis.

The modeled intensity spectrum was calculated only for the most interesting film in terms of color effects – 1000 nm SiO_2 on Silicon (Fig. 19).

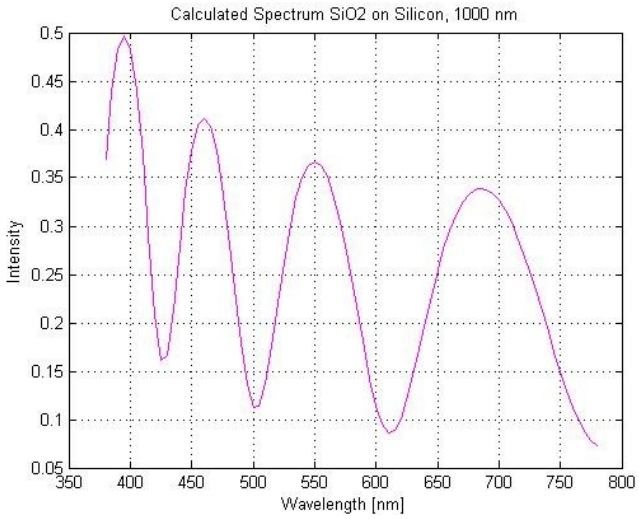

Fig. 19: Calculated optical spectrum – thick film SiO_2 on Silicon, 1000 nm, the dependence of the total intensity on the wavelength

Compared to the measured spectra obtained from the ellipsometer, there is almost no difference between the modeled and measured spectra (Fig. 20). Note that for the purpose of this thesis we restrict the spectral range in Fig. and Fig. to the visible region.

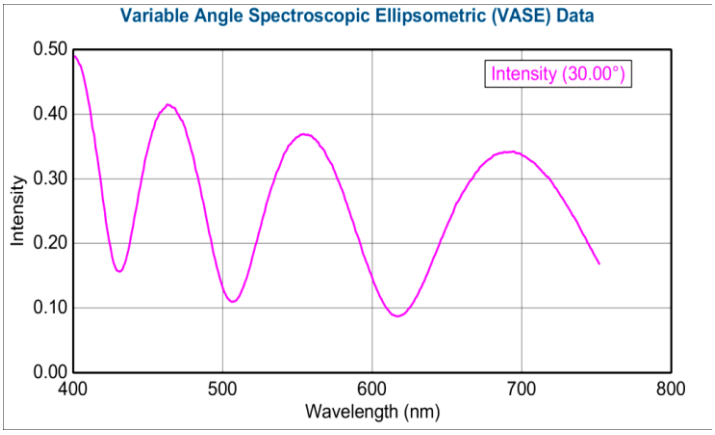

Fig. 20: The measured spectrum of the thick film SiO_2 on silicon, 1000 nm, at the angle of incidence of 30°.

To compare the intensity spectra of a thin and a thick layer, the measured spectra are plotted in one graph (Fig. 21).

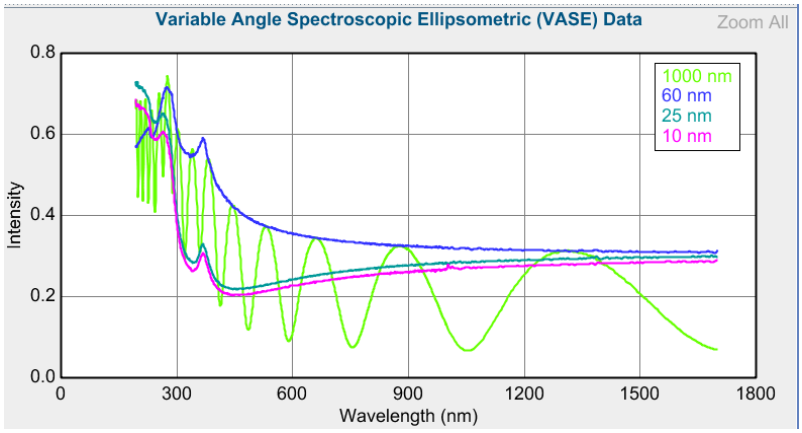

Fig. 21: Measured intensity spectra of thin films with thickness of 1000 nm, 60 nm, 25 nm and 10 nm at the angle of incidence of 40° - comparison.

Then we can see that the intensities vary quite a lot and so the color effects are the best to calculate on the 1000 nm thick layer.

4.5.1 Calculation of the Spectrum for s- and p- Polarization of the Measured Data

As we are measuring reflectivity – intensity spectrum on the ellipsometer, we have obtained values of the total intensity of light

$$R = \frac{1}{2}(Rs + Rp) \tag{4.9}$$

Calculation of the intensity coefficients from the amplitude reflection coefficients is defined as

$$R_{s,p} = \left|r_{s,p}\right|^2, \frac{Rp}{Rs} = tan^2\Psi. \tag{4.10}$$

Ψ and R are known from the exported measured data. Furthermore, we derive formulas for calculation of Rs and Rp intensity reflection coefficients.

$$2R = Rs \cdot \frac{1}{cos^2\Psi},\ Rs = 2Rcos^2\Psi,\ Rp = 2R(1 - cos^2\Psi),\ Rp = 2Rsin^2\Psi \tag{4.11}$$

4.5.2. Calculated Trichromatic Coordinates – Color Coordinates

The color coordinates calculated for the SiO_2 on Si, 1000 nm thick film are shown in the following graphs as a function of the angle of incidence (Fig. 22, Fig. 23). The coordinates calculated from the measured data are compared to those calculated from the modeled optical spectra of the thick film. Calculated CIE x, y, z trichromatic coordinates from both spectra (Fig. 22) are transferred to CIE r, g, b trichromatic coordinates (Fig. 23).

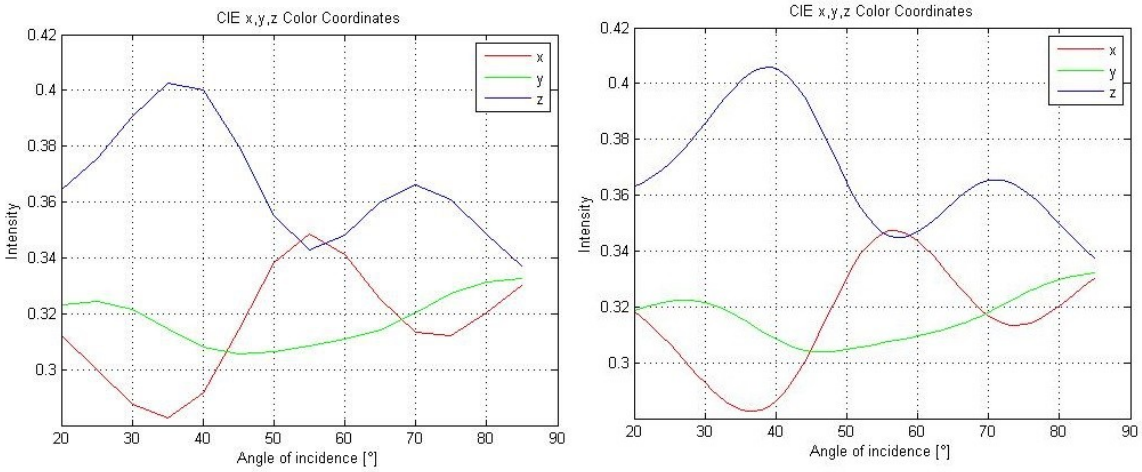

a) b)

Fig. 22: Calculated CIE x,y,z trichromatic coordinates of SiO_2 on Si, 1000 nm thick film a) from modeled optical spectra, b) from measured optical spectra.

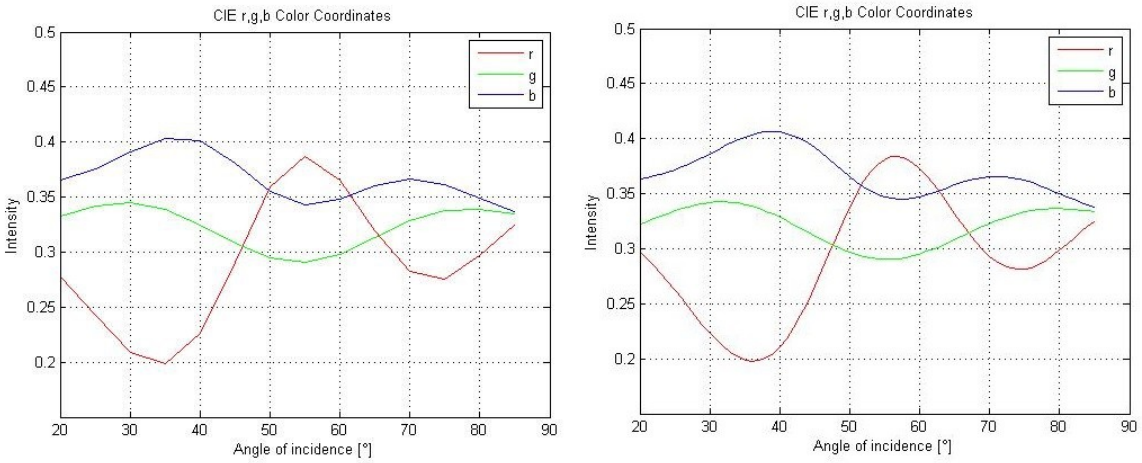

a) b)

Fig. 23: Transformed CIE r,g,b, trichromatic coordinates of SiO_2 on Si, 1000 nm thick film a) from modeled optical spectra b) from measured optical spectra.

The modeled trichromatic coordinates of thin films with different thickness are plotted in the chromaticity diagram shown in Figure (24). The modeled 1000 nm thick film has a black color in the diagram, 500 nm is represented with a green color, 250 nm with blue and 100 nm with yellow.

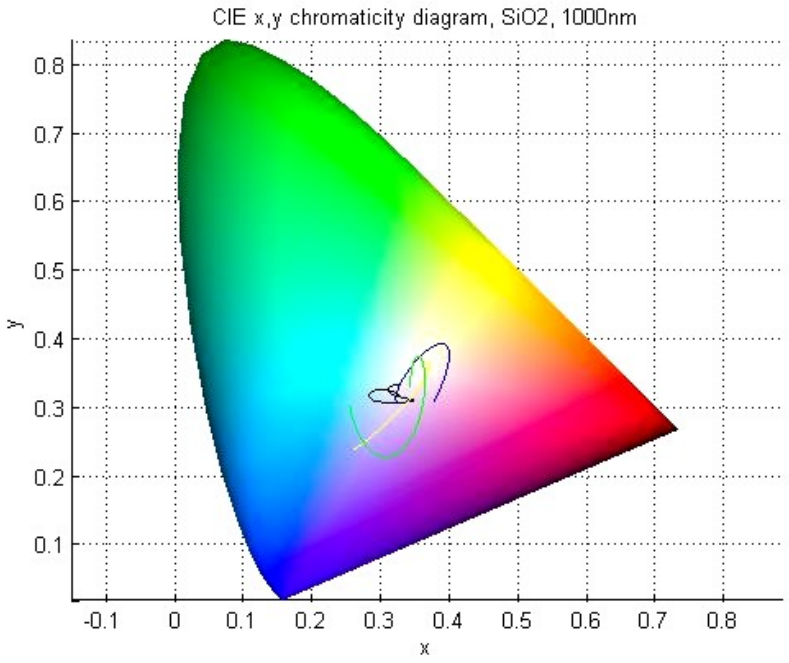

Fig. 24: Calculated x, y chromaticity coordinates of thin films with various thickness plotted in the chromaticity diagram.

The picture of the measured 1000 nm SiO_2 thick film is shown in Fig. 25. The colors vary with the viewing angle.

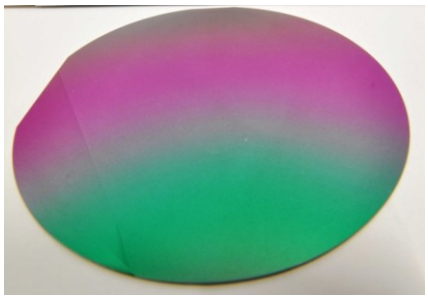

Fig. 25: Measured 1000 nm SiO2 on Silicon thick film

The dependence of the thin film thickness to the angle of incidence is shown in Figure 26. The right side represents the 1000 nm thick film and the left side represents the wafer.

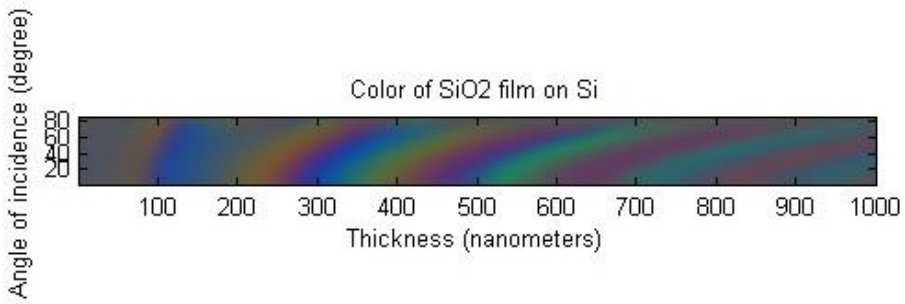

Fig. 26: Color dependence of thickness of thin films to an angle of incidence

5. CONCLUSION AND DISCUSSION

The main result of this bachelor thesis are calculations of the trichromatic coordinates from the measured and modeled optical spectra of the SiO_2 on Si 1000 nm thick film and from a given emission spectra of the gasses causing the aurora phenomenon in the atmosphere. Both coordinates are calculated for RGB and CIE XYZ color space. The thin film color coordinates are presented in Figure 22, 23, 24, and 26. The coordinates calculated from aurora are shown in Figure 13, 14, 15, and 16.

I would like to continue working with color effects because of its wide applications and perspective. One of the perspectives is an application of colorimetry for description of color effects in specially designed periodic structures, for example, in the frame of collaboration with Optaglio Company to design holograms with unusual color effects.

REFERENCES

[1] GARCÍA, SOLÉ, J., BAUSÁ, L., JAQUE, D. *An Introduction to the Optical Spectroscopy of Inorganic Solids*. 1st ed. John Wiley & Sons, 2005. 304 p. ISBN 04-708-6886-4.

[2] HOLLAS, J. *Modern Spectroscopy*. 4th ed. John Wiley & Sons, 2004. 452p. ISBN 04-708-4416-7.

[3] HAVELKA, B. *Geometrická optika*. 1st ed. Prague, 1956. 286 p.

[4] MALACARA, D. *Color Vision and Colorimetry: Theory and Applications.* 2nd ed. SPIE Press, 2002. 164 p. ISBN 08-194-4228-3.

[5] HUNT, R., POINTER, M., MALACARA, D. *Measuring Colour: Theory and Applications*. 4th ed. John Wiley & Sons, 2011. 469 p. ISBN 978-1-119-97559-5.

[6] POSTAVA, K. Spectroscopy of Nanostructures: *„1. Instrumentation – spectrometers" lecture.* Ostrava, VŠB – Technical University of Ostrava, Institute of Physics, 2012.

[7] Explanation of Various Light Sources and Their Use in Visual Color Matching Applications, 2004. GTI Graphic Technology, Inc., http://www.gtilite.com/gti-pdf/Various-Light-Sources.PDF (accessed April 28, 2014).

[8] CIE, Commission Internationale de l'Eclairage, *Colorimetry*. 3rd ed. Saint-Gobain Recherche Documentation, 2004. 79 p. ISBN 3901906339.

[9] The Florida State University: National High Magnetic Field Laboratory; Sources of Visible Light, 2003. Molecular Expressions. http://micro.magnet.fsu.edu/primer/lightandcolor/lightsourcesintro.html (accessed April 28, 2014).

[10] MORTIMER, R.J., VARLEY, T.S. Quantification of colour stimuli through the calculation of CIE chromaticity coordinates and luminance data for application to in situ colorimetry studies of electrochromic materials. *Displays* [Online] 2011, vol. *32*, 35-44. http://www.sciencedirect.com/science/article/pii/S014193821000079X (accessed April 28, 2014).

[11] University of South Carolina, School of Medicine, Color Models CIEXYZ, 2000. Technical Guides. http://dba.med.sc.edu/price/irf/Adobe_tg/models/ciexyz.html (accessed April 28, 2014).

[12] KRATOCHVÍL, T., MELO, J. Utilization of Matlab for TV Colorimetry and Color Spaces Analysis. In *Technical Computing Prague 2006 14th Annual Conference Proceedings*; , 1st ed., ICT Prague Press, 2006. 53–60. ISBN: 80-7080-616- 8.

[13] MCGAVIN, D., STUKENBORG, B., WITKOWSKI, M. Color Figures in BJ: RGB versus CMYK. *Biophys. J.* [Online] 2005, vol. *88*, 761-762. http://www.ncbi.nlm.nih.gov/pmc/articles/PMC1305152/ (accessed April 28, 2014).

[14] SUDHAKARAN, S. What is Color Space and the Tristimulus Values XYZ?, 2013. wolfcrow. http://wolfcrow.com/blog/what-is-color-space-and-the-tristimulus-values-xyz/ (accessed April 28, 2014).

[15] POSTAVA, K. Physics III – Optics: „*B. Skalární vlnová optika" lecture*, Ostrava, VŠB – Technical University of Ostrava, Institute of Physics. 2013.

[16] SALEH, E.A.B., Teich, M.C. *Fundamentals of photonics*. 2nd ed. John Wiley & Sons, 1991. 966 p. ISBN 04-718-3965-5.

[17] KÖNNEN, G. *Polarized light in nature*. 1st ed. Cambridge University Press, 1985. 196 p. ISBN 05-212-5862-6.

[18] Leon, N. What causes a rainbow?, 2013. SciJinks. http://scijinks.jpl.nasa.gov/rainbow (accessed April 28, 2014).

[19] Tržický, T. Introduction to Halo Effects, 2014. Optics of the Atmosphere. http://ukazy.astro.cz/halo.php (accessed April 28, 2014).

[20] KUHN, T. Arctic Science: *„ Ice particles in the atmosphere" lecture*, Kiruna, Umea University, Swedish Institute of Space Physics, 6 Feb 2013.

[21] Synaková, L. Optické jevy v přírodě. Bachelor thesis, Masaryk Univeristy, School of Medicine, Brno, 2006.

[22] Calvert, J. The Halo, 2003. Dr James B. Calvert. http://mysite.du.edu/~jcalvert/astro/halo.htm#Refs (accessed April 28, 2014).

[23] University of Wisconsin – Madison. Iridescent Clouds, 2013. Cooperative Institute for Meteorological Satellite Studies. http://cimss.ssec.wisc.edu/wxwise/class/iredsnce.html (accessed April 28, 2014)

[24] KUNČICKÁ, Š. *Assignment 2 2013: Problem Sheet*. Umea, Umea University, Department of Physics. 2013.

[25] Hinz, C. Atmospheric phenomena. Polar Stratospheric Clouds, 2014. Arbeitskreis Meteore e.V. http://www.meteoros.de/psc/psce.htm (accessed April 28, 2014).

[26] University of Illinois: Department of Atmospheric Sciences Coronas, 2010. WW2010: the weather world 2010.

http://ww2010.atmos.uiuc.edu/(Gh)/guides/mtr/opt/wtr/coro.rxml (accessed April 28, 2014).

[27] NORBERG, C. *Aurora Borealis Practical, Arctic Science course 2013*. Kiruna, Umea University, Department of Physics. 2010.

[28] Jutström, J. Why are there auroras?, 2013. Swedish Institute of Space Physic. http://www.irf.se/norrsken/Norrsken_why.html (accessed April 28, 2014).

[29] Zawischa, D. Atomic spectra, 2013. Institute for Theoretical Physic. https://www.itp.uni-hannover.de/~zawischa/ITP/atoms.html (accessed April 28, 2014).

[30] NORBERG, C. „*The Physics of the Aurora Continued", Aurora_Presentation2_AS2013, lecture. Arctic Science course 2013*. Kiruna, Umea University, Department of Physics, 2013

[31] HARGREAVES, J. *The solar-terrestrial environment: an introduction to geospace – the science of the terrestrial upper atmosphere, ionosphere, and magnetosphere.* 2nd ed. Cambridge University Press, 1995, 420 p. ISBN 05-214-2737-1.

[32] SANDAHL, I., SERGIENKO, T., BRÄNDSTRÖM, U. Fine structure of optical aurora. *Journal of Atmospheric and Solar-Terrestrial Physics* [online]. 2008, vol. 70, no. 18 [cited 2014-04-28], p. 2275–2292. Available from http://www.sciencedirect.com/science/article/pii/S1364682608002162 .

[33] DEMPSEYX, J.T., Storey, J.W.V. & Phillips, M.A., Auroral Contribution to Sky Brightness for Optical Astronomy on the Antarctic Plateau, 2005. *Publications of the Astronomical Society of Australia*. 2005, vol. 22, is 02, p. 91-104.

[34] Kari, K. Optical measurements of aurora, 2011. University of Oulu, Department of Physics. http://kho.unis.no/misc/AGF351/Lectures/Kari_Aurora_Spectroscopy.pdf (accessed April 28, 2014).

[35] OHRING, M. *Materials Science of Thin Films*. 1st ed. Elsevier Science & Technology Books, 1991. 750 p. ISBN 012524990X.

[36] FOX, M. *Optical Properties of Solids*. 1st ed. Oxford University Press, 2001, xii, 305 P. ISBN 978-0-19-850612-6.

[37] HEAVENS O., S. *Optical Properties of Thin Solid Films*. 2nd ed. Dover Publications, Inc., 1955. 288 p. ISBN 0486669246.

[38] STENZEL, O. *The Physics of Thin Film Optical Spectra: An Introduction*. 1st ed. 2005. Springer, 2005. 277 p. ISBN 35-402-3147-1.

[39] FUJIWARA, H. *Spectroscopic Ellipsometry: Principles and Applications*. John Wiley & Sons, 2007. 369 p. ISBN 978-0-470-01608-4.

[40] GARCIA-CAUREL, E., OSSIKOVSKI, R., FOLDYNA, M., PIERANGELO, A., DRÉVILLON, B., DE MARTINO, A. Advanced Mueller Ellipsometry Instrumentation and Data Analysis. Ellipsometry at the Nanoscale. Springer Berlin Heidelberg, 2013. 31 p.

[41] LOSURDO, M., BERGMAIR, M., BRUNO, G., CATTELAN, D., COBET, Ch., MARTINO, A., FLEISCHER, K., DOHCEVIC-MITROVIC, Z., ESSER, N., GALLIET, M., GAJIC, R., HEMZAL, D., HINGERL, K., HUMLICEK, J., OSSIKOVSKI, R., V. POPOVIC, Z. and SAXL, O. Spectroscopic ellipsometry and polarimetry for materials and systems analysis at the nanometer scale: state-of-the-art, potential, and perspectives. *Journal of Nanoparticle Research* [Online] 2009, *11*, 1521-1554. http://link.springer.com/article/10.1007%2Fs11051-009-9662-6 (accessed April 28, 2014).

[42] POSTAVA, K. *Thin Films*, *lecture*, Ostrava, VŠB – Technical University of Ostrava, Institute of Physics. 2013.

[43] POSTAVA, K. Physics III – Optics: „*C. Electro-optics" lecture*, Ostrava, VŠB – Technical University of Ostrava, Institute of Physics. 2013.

[44] Ellipsometry Measurements, 2014. J.A. WOOLLAM CO. INC. http://www.jawoollam.com/tutorial_4.html (accessed April 28, 2014).